Submitted to Science

Cosmological Deuterium Abundance and the Baryon Density of the Universe

SCOTT BURLES[1] & DAVID TYTLER[1]
Department of Physics, and Center for Astrophysics and Space Sciences
University of California, San Diego
C0111, La Jolla, CA 92093-0111

ABSTRACT

Standard big bang nucleosynthesis (BBNS) promises accurate predictions of the primordial abundances of deuterium, helium-3, helium-4 and lithium-7 as a function of a single parameter. Previous measurements have nearly always been interpreted as confirmation of the model (1). Here we present a measurement of the deuterium to hydrogen ratio (D/H) in a newly discovered high redshift metal-poor gas cloud at redshift $z = 2.504$. This confirms our earlier measurement of D/H (2), and together they give the first accurate measurement of the primordial D abundance, and a ten-fold improvement in the accuracy of the cosmological density of ordinary matter. This is a high density, with most ordinary matter unaccounted or dark, which is too high to agree with measurements of the primordial abundances of helium-4 and lithium-7. Since the D/H measurement is apparently simple, direct, accurate and highly sensitive, we propose that helium requires a systematic correction, and that population II stars have less than the primordial abundance of ^{7}Li. Alternatively, there is no concordance between the light element abundances, and the simple model of the big bang must be incomplete and lacking physics, or wrong.

In the standard big bang model the primordial abundances of the light elements depend on the unknown value of the cosmological baryon (ordinary matter) to photon ratio, η (1,3–5). A measurement of primordial D/H, which is very sensitive to η, leads to precise predictions for the abundances of the other light elements, which can be compared with observations to test the model.

---

[1]Visiting Astronomer, W. M. Keck Telescope, California Association for Research in Astronomy

Unfortunately D is destroyed inside stars, which then eject gas with H but no D. As more gas is processed and ejected, the value of D/H in the interstellar medium of our Galaxy drops further below primordial. We look for primordial D/H in quasar absorption systems (QAS) (6,7), some of which sample gas at early epochs, and in intergalactic space where there are too few stars to destroy significant amounts of D.

The absorption system at $z = 2.504$ towards QSO 1009+2956 was from 40 QSO spectra which we obtained at Lick Observatory because it showed a steep Lyman limit break and weak metal lines, which indicate a low b-value suitable for the detection of deuterium. Of the 15 QSOs which met these criteria and were subsequently observed with the 10-m W. M. Keck telescope, only 2 have yielded deuterium measurements (8). We now describe a measurement of D/H, in this new QAS, which agrees with our previous low value, but not with measurements of a high D/H (9,10). Either BBNS was inhomogeneous (11) and D/H varies spatially, or more likely, the spectra showing high D/H were contaminated.

In Figure 1 we show nine lines in the absorption system at $z = 2.504$ towards QSO 1009+2956. All six metal absorption lines are best fit by two components separated by 11 km s^{-1}, using the parameters given in Table 1. The dotted lines show the expected positions of the H and D lines for the gas at the well determined redshifts of these components. The two components adequately fit the blue side of the Lyman features, but an extra H component at $v_{rel} = +40$ km s^{-1} is seen on the red side which is not significant in our measurement of D/H.

The D Lyman-α absorption is unsaturated and has a well determined total column density, N(D I). However the amount of D in the red component is not well determined because it is blended with both the blue D and H components. If we do not include the red D component, systematic under-absorption would occur at that velocity, so we set $(D/H)_{red}=(D/H)_{blue}=(D/H)_{total}$.

All lines from the same gas will have the same turbulent velocity dispersions b_{tur}, but the thermal widths will depend on the mass of each ion: $b_{therm} = 0.128\sqrt{T m_p/m_{ion}}$ km s^{-1} , where m_p is the proton mass. We use the b-values of Si, C, and H in Table 1 to obtain the temperatures and b_{tur} of the two components. These values are consistent with a single b_{tur} for all lines, and allow us to calculate that the red component of D should have b(D I) $= \sqrt{b_{therm}^2 + b_{tur}^2} = 15.4$ km s^{-1} which we use as a constraint on the fit because we cannot measure this value from the D line. The widths of the H and D lines are dominated by thermal motions, so the lines are accurately fit by Voigt profiles (2,12). A simultaneous fit to the Lyman α, β, and γ lines in the Keck spectrum and the Lyman continuum absorption in the Lick spectrum (Figure 2) gives D/H $= 3.0\,^{+0.6}_{-0.5} \times 10^{-5}$ (1σ random photon and fitting errors).

A systematic increase in D/H comes from the chance superposition of weak H absorption at the expected position of D. To estimate this, we made noise-less model spectra with D and H lines at the redshifts given by the metal lines. We used the b values and N(H I) from Table 1, but we vary N(D I). For each N(D I) we made 10^6 spectra, and to each of these we added random lines to simulate the Lyα forest, using the known distribution of z, N(H I) and b-values for forest lines (13). We then calculated the likelihood that the data came from the model spectra for each D/H. Assuming that all values of D/H are equally likely *a priori*, the expected or mean D/H is Log $(\mathrm{D/H})_{exp} = -4.60\,^{+0.02}_{-0.04}$, where the errors are the standard deviations of the likelihood distribution above and below the mean. The correction from the Monte Carlo simulations changes our value from a formal upper limit to a measurement of D/H. Additional systematic errors in D/H from fitting the continuum level are estimated to be ΔLog (D/H) = 0.06. We varied the continuum by 2% near Lyα (Figure 1), and by 10% near the Lyman continuum (Figure 2), and for each combination we re-fit the spectra. Including the uncertainties due to systematics, we find

$$Log\left(\frac{D}{H}\right) = -4.60 \pm 0.08 \pm 0.06 \tag{1}$$

where the errors represent the 1σ random error followed by the systematic errors from the continuum level.

The blue side of the blue D Lyα line appears unblended, and is fit with b(DI) = 15.7 $\pm$ 2.1 km s^{-1}. This is consistent the value of $b = 13.5 \pm 0.5$ km s^{-1} predicted from the b_{therm} and T given by the metal and H lines. Less than 2% of H Lyα lines have b-values this small or smaller (13), so it is unlikely that this line is strongly contaminated with H. Metal lines can be this narrow, although they are usually narrower with $b < 10$ km s^{-1}. The D feature is unlikely to be a metal line because metal lines of this strength are nearly always accompanied by other lines, and the spectra has been searched for these lines. The *a posteriori* probability of a random H line with $b < 17.8$ and $N > 12.6$ cm^{-2}, to account for > 0.5 of the D line, and redshift within 20 km s^{-1} of that of the metal lines is $< 8 \times 10^{-4}$. A high correlation of "satellite" components on these velocity scales could increase the probability by as much as a factor of 3 (7,13).

The residual flux below the Lyman edge gives an accurate measure of all H I in this velocity region (Figure 2, 14). There are no other Lyα lines within 5000 km s^{-1} of $z = 2.50$ which have H I column densities $> 10^{16}$ cm^{-2}, so that all of the Lyman continuum absorption must be produced by gas in the $z = 2.504$ absorption system. The blue side of the Lyα , Lyβ and Lyγ lines are best fit if all of this H I is near the two velocity components which are seen in the metals. There could be be additional H at velocities between the metal lines and +40 km s^{-1} , provided this gas has very low metal abundances ([C/H]

< -3.5). However, nearly all known QAS with large N(H I) have metal abundances [C/H] > -3.

The column densities of the metals and neutral hydrogen give the metallicity and neutral fraction of the gas. Following Donahue & Shull (15), we model the system as an optically thin gas ionized by a typical QSO photoionizing spectrum given by Mathews & Ferland. We estimate the ionization parameter (the ratio of the number of photons with energies above one Rydberg to the number of atoms): U $\equiv n_\gamma/n_p \approx 10^{-2.8}$, which gives the metal abundances shown in Table 1. For a photoionization model of low metallicity components, this corresponds to a neutral hydrogen fraction of H I/H $\approx 10^{-2.5}$.

The measured D/H is consistent with normal Galactic chemical evolution (2,16); the destruction of D in known populations of stars can account for our D/H, that in the per-solar nebula, and the current ISM D/H. In the ISM, D/H $= 1.6 \pm 0.1 \times 10^{-5}$ (17), for [O/H] = -0.25. If the destruction of D is proportional to [O/H], then we would expect 0.005 of the D would be destroyed for [O/H] < -2.5 (18).

We find [C/Si] $\simeq -0.3$ in both components which is characteristic of low metallicity stars in the halo of our Galaxy. This suggests that the C and Si were created in "normal" supernovae. If some additional astrophysical processes destroys D, it must do so without producing more C and Si than we see, or other elements which we would have seen if they were made, and without changing the usual C/Si ratio. If primordial D/H were 24×10^{-5} (9,10) then 87% of D must be destroyed in Q1009+2956 and 90% in Q1937−8118. The level of destruction would be large and similar for [C/H] = -3.0 to -2.2, but small for Q0014+8118 with [C/H] < -3.5. Redshift is apparently not a factor.

The QAS towards Q1937-1009 in which we previouly measured a low D/H is extremely similar to Q1009+2956, except that N(H I) is larger, and the redshift is higher (2). We used the Lyman series lines up to 19, and the absence of flux in the Lyman continuum to constrain the N(H I), and we obtained smaller errors: Log D/H $= -4.64 \pm 0.06 \pm 0.06$.

The best estimate of the primordial D/H is obtained by taking the average of our two measurements weighted by the squares of their random errors:

$$Log\left(\frac{D}{H}\right) = -4.62 \pm 0.05 \pm 0.06, \tag{2}$$

where the first error is the random error on the weighted mean, and the second is the larger of the systematic errors from the continuum level uncertainty. We do not add these systematic errors because they have a similar origin and the two measurments agree to within the random errors: Prob($\chi^2 \geq 0.18$) = 0.67. In linear units, the mean is

$$\left(\frac{D}{H}\right) = 2.4 \pm 0.3 \pm 0.3 \times 10^{-5} \tag{3}$$

In Table 2 we list all published measurements of D/H in QAS. Only the two discussed above are measurements. The others were initially presented as limits or possible detections, and they will all be biased to higher than true D/H because they do not include corrections for weak H at the position of D.

The QAS towards Q0014+8118 differs from our two in several ways. Since no metal lines were detected, the velocity structure of the cloud could be determined only by median filtering of the higher-order lines in the Lyα forest (9). The Lyman-α feature was considerably more complex: five components were required for an adequate fit (instead of three), with two components within 30 km s^{-1} of the deuterium absorption line (10). The neutral hydrogen column density of the component where deuterium is measured, Log N(H I) = 16.74, is 4 and 10 times lower than the column densities in our two QAS, which reduces the sensitivity to low D/H.

Rugers & Hogan reanalyzed the published spectra of Q0014+8118, and determined that the deuterium feature is better fit with two very narrow components separated by 21 km s^{-1} (19). They claim that it is very unlikely that there are two narrow lines by chance at the expected position of D, but we are not convinced because there are no metal lines to constrain the velocities and their model is a poor fit to the data in many places (20). These data remain consistent with this D line being contaminated (21).

Towards QSO 1202-0725, Wampler et al. (22) find $D/H < 15 \times 10^{-5}$ at a redshift $z = 4.672$. This QAS has high metallicity, [O/H] = 0.3, and does not look suitable for inferences of primordial D/H. Towards QSO 0420-3851, Carswell et al. (23) find a lower limit of $D/H > 2 \times 10^{-5}$ at $z = 3.086$. This QAS also has a high metallicity, [O/H] = -1.0. The D I column is fairly well-determined, but the H I is high, N(H I) $> 10^{18}$ cm^{-2}, and is very uncertain. All data in Table 2 are consistent with our low D/H value, but our data are inconsistent with high D/H, unless D/H is distributed inhomogeneously (11).

We now discuss the baryon density implied by our low D/H measurements. In Figure 3 we show how D/H fits into the standard cosmological framework. For the remainder of this paper, we present the implications of the new D/H measurements on these quantities. The current cosmological density of baryons, ρ_b, is given by

$$\eta = 6.4\,^{+0.5}_{-0.4}\,^{+0.6}_{-0.5}\,^{+0.3}_{-0.3} \times 10^{-10}, \tag{4}$$

where the third error is the 1σ from nucleosynthesis predictions (5). The density of photons from the Cosmic Microwave Background (24), $n_\gamma = 411\, cm^{-3}$ gives:

$$\rho_b \equiv \eta\, n_\gamma\, m_p = 4.4\ \pm 0.3\ \pm 0.4\ \pm 0.2 \times 10^{-31}\, g\, cm^{-3}, \tag{5}$$

and as a fraction of the current critical density, $\rho_c = 3H_0^2/8\pi G$,

$$\Omega_b \equiv \frac{\rho_b}{\rho_c} = 0.024\ \pm 0.002\ \pm 0.002\ \pm 0.001\, h^{-2} \tag{6}$$

where the Hubble constant, $H_0 = 100\, h$ km s^{-1} Mpc^{-1}. Since the observed density of visible baryons in stars and hot gas is about $\Omega_{LUM} = 0.003$ (25), most baryons (about 94% for $h = 0.7$) are unaccounted.

In Figures 4–6, we present the predicted adundances of ^{4}He, ^{3}He and ^{7}Li relative to hydrogen (5). We show values of η in the shaded region which are consistent with our D/H. The usually accepted estimates of primordial ^{4}He come from measurements of low-metallicity extragalactic H II regions. Even modest chemical production can significantly change the abundance of ^{4}He, so the primordial value is inferred by extrapolating ^{4}He measurements to zero metallicity (26–28). Pagel et al. reported an inferred primordial mass fraction of ^{4}He, $Y_p = 0.228 \pm 0.005$, with a 95% upper bound of 0.242 including systematic errors (26). Recently, Thuan et al. found $Y_p = 0.241 \pm 0.003$ (28).

These ^{4}He measurements are not consistent with our D/H, which predicts

$$Y_p = 0.249 \pm 0.001\ \pm 0.001\ \pm 0.001. \tag{7}$$

To quantify the discordance of D/H with the ^{4}He measurements mentioned above, we form the weighted mean η using our mean D/H and either of the ^{4}He values. We weight with the random errors alone, where we now include nuclear uncertainties in quadrature in our D/H error. We find Prob($\chi^2 > 5.2$) = 0.02 for the low Y_p, and Prob($\chi^2 > 3.0$) = 0.08 for the high Y_p. If BBNS is correct, this disagreement shows that there must be systematic errors which should be identified and corrected. Reducing our D/H by its systematic error, gives Prob($\chi^2 > 3.7$) = 0.05 for the low Y_p shifted up by its systematic error, and Prob($\chi^2 > 2.7$) = 0.1 for the high Y_p, which does not have a quoted systematic error. Even with the allowances of current systematic error estimates, D/H and Y_p fail to predict the same value of η with BBNS.

^{3}He is more complex and poorly understood because it is both created and destroyed in stars. The ratio of the D mass fraction in the ISM to primordial D is $X_{D(ISM)}/X_{D0} = 0.67 \pm 0.09$ (random, not systematic error). If ^{3}He undergoes the same amount of destruction, then its primordial abundance would be 1/0.67 times that in the ISM, which is an upper limit because ^{3}He is also created (e.g. primordial D is burned in stars to make ^{3}He). Low mass stars may produce ^{3}He copiously (29), as is suggested by its high abundance in the ejecta of planetary nebulae (30). If this is the case, only upper limits on ^{3}He, not D + ^{3}He, can be correctly applied to cosmology. However the observed abundance in Galactic H II regions is 5 – 20 times lower than expected (31), for unknown reasons, perhaps because some of the ^{3}He made in low mass stars is later destroyed, or because observations are made in H II regions which contain the ejecta of high mass stars which destroy ^{3}He (32).

The abundance of ^{7}Li in stars in the disk of our Galaxy (population I) spans three orders of magnitude, because Li is both made (e.g. by cosmic ray spallation in the interstellar medium, and in novea and supernovae) and destroyed, but warm metal-poor halo (population II) stars have similar "plateau" abundances of ^{7}Li in their atmospheres. These measurements (33-35), shown in Figure 6, are often taken as the primordial abundance, but recent data show that this is not justified. Stars with very similar temperatures and metallicities, subgiant stars in the globular cluster M92, and turnoff stars in the halo, have significantly different ^7Li abundances (36), perhaps because of different amounts of ^{7}Li depletion. Ryan et al. have found that the ^{7}Li abundance depends on both temperature and metallicity in ways which were not predicted and are not understood. If we are to obtain a primordial ^{7}Li abundance we must either (1) understand why its abundance varies from star to star, and learn to make quantitative predictions of the level of depletion, or (2) make measurements in relatively unprocessed gas. Our D/H measurements imply that ^{7}Li in population II stars has been depleted by about 0.5 dex, which may be difficult to reconcile with the near constancy of ^{7}Li in the warm halo stars.

We conclude that our D/H measurements are probably the first measurements of a primordial abundance ratio of any elements, and that they give about an order of magnitude improvement in the accuracy of estimates of ρ_b.

Where are the baryons? The MACHO collaboration recently announced detection of baryonic dark matter in the halo of our Galaxy from 7 microlensing events towards the Large Magellanic Cloud (37). The most likely mass of the MACHOs is 0.3 - 0.5 solar masses, from the durations of the events and the velocities implied by the model of the halo of our Galaxy. This corresponds to a standard halo model mass of $1.6\times10^{11}\ M_{\odot}$, and a large fraction of the total mass. If the halos in all galaxies are entirely baryonic MACHOS, they have $\Omega_{MACHO} > 0.13$ (90% confidence, with prefered values exceeding 0.3 for h=0.75 38). This is more than $\Omega_b = 0.043 \pm 0.009$, which is predicted from our two measurements, so < 0.5 (prefered value 0.16) of halos are baryonic. The MACHO detections strongly imply a high Ω_b: if halos are 50% baryonic MACHOS then $\Omega_b > 0.065$ (90% confidence for h=0.75), enough to account for all baryons.

X-ray observations reveal that baryons in the form of hot gas contribute a fraction $f_x = (0.05 - 0.14)\, h^{-3/2}$ of the total mass of clusters of galaxies (39). The remaining mass is some combination of unseen dark baryons (e.g. MACHOS) and any other non-baryonic dark matter, such as massive supersymmetric particles. The baryon fraction in clusters is then $f_b \geq f_x$. Since galaxy clusters are the largest bound structures in the universe, their f_b should provide good estimates of the cosmological value, so the total mass density of the universe is then:

$$\Omega_{total} = \Omega_b / f_b \leq (0.14 - -0.58)\, h^{-1/2}, \tag{8}$$

where we used Ω_b from D/H and the inequality allows for $f_b \geq f_x$ (40). Although our D/H measurements give a very high Ω_b, it is not high enough to permit $\Omega_{total} = 1$ from matter: we have $\Omega_{total} < 0.72$ from $\Omega_b = 0.029\, h^{-2}$, $h = 0.6$, and $f_b = f_x$. Either the universe is open, as is now allowed by the theory of inflationary cosmology $\Omega_{total} \leq 1$ (41), or there is a cosmological constant.

We are forced to conclude, given the present state of primordial abundance measurements, that D/H gives the only reliable constraints on η and Ω_b. The practice of finding consensus among all the light elements should be heavily weighted to D/H, because it is most sensitive to η, and because of the apparent absence of systematic uncertainties arising from destruction and creation. The discordance with other light elements does not demand alternative models to the standard big-bang, rather it begs for all measurements of primordial abundances to be made in similar pristine sites. The search for more deuterium measurements in QAS will continue, and at the current rate, $\Omega_b\, h^2$ is likely to be known to 5% by the end of the millenium.

Ion	Blue Component	Red Component	Total
H I	N = 17.36 ± 0.09	N = 16.78 ± 0.11	N = 17.46 ± 0.05
	b = 18.8 ± 0.5	b = 21.9 ± 4.1	
D I	N = 12.84 ± 0.09	N = 12.26*	N = 12.94 ± 0.06
	b = 15.7 ± 2.1	b = 15.4#	
Si III	N = 12.81 ± 0.06	N = 12.55 ± 0.04	N = 13.00 ± 0.03
	b = 4.9 ± 0.4	b = 4.8 ± 0.8	
Si IV	N = 12.50 ± 0.03	N = 12.05 ± 0.08	N = 12.63 ± 0.02
	b = 4.9 ± 0.6	b = 3.9 ± 1.5	
C II	N = 12.46 ± 0.12	N = 12.18 ± 0.18	N = 12.64 ± 0.08
	b = 7.0 ± 3.2	b = 3.7 ± 4.2	
C IV	N = 12.81 ± 0.04	N = 12.56 ± 0.06	N = 13.00 ± 0.03
	b = 5.4 ± 0.6	b = 5.6 ± 1.2	
T(10^4 K)	2.1 ± 0.1	2.4 ± 0.7	
b_{tur}	3.2 ± 0.4	2.3 ± 1.4	
[C/H]	−2.9	−2.8	...
[Si/H]	−2.5	−2.6	...
[C/Si]	−0.4	−0.2	...

Table 1: Model parameters for QAS at $z = 2.504$ towards Q1009+2956. Column densities (N) are in logarthmic units of cm^{-2}, while the b-values are in units of km s^{-1} .

*We fixed this column density to make D/H the same value in both components.

#This b-value is calculated from the most likely turbulent velocity and temperature of the red component.

QSO	z_{abs}	D/H$\times 10^5$	1σ *	logN(H I)	[C/H]#	Reference
ISM	0.0	1.6	0.1	18.2	...	17
1009+2956	2.504	2.5	0.5	17.46	–2.9	This Paper
1937−1009	3.572	2.3	0.3	17.94	−2.2, −3.0	2
0014+8118	3.320	$\leq 19 - 25$	...	16.7	< -3.5	9,10,19
1202−0725	4.672	≤ 15	...	16.7	...	22
0420−3851	3.086	≥ 2	...	≥ 18	-1.0	23

Table 2: Recent Measurements of D/H

*approximate standard deviation on D/H measurement

#Carbon to hydrogen ratio in logarthimic units, relative to solar

REFERENCES

1. C. J. Copi, D. N. Schramm, M. S. Turner, *Science* **267**, 192 (1995).

2. D. Tytler, X-M. Fan, S. Burles, Submitted to *Nature* (1996).

3. R. V. Wagoner, W. A. Fowler, F. Hoyle, *Astrophys. J.* **148**, 3 (1967); J. Yang, M. S. Turner, G. Steigman, D. N. Schramm, K. A. Olive, *ibid.* **281**, 493 (1984); K. A. Olive, D. N. Schramm, D. Thomas, T. P. Walker, *Phys. Lett. B* **236**, 454 (1990). By standard BBN, we assume spatial homogeneity, three light neutrino species with vanishing chemical potentials, and no additional light particles present in thermal abundance.

4. T.P. Walker, G. Steigman, D. N. Schramm, K. A. Olive, H. S.Kang, *Astrophys. J.* **376**, 51 (1991); M. S. Smith, L. H. Kawano, R. A. Malaney, *Astrophys. J. Suppl. Ser.* **85**, 219 (1993).

5. S. Sarkar submitted to *Rep. on Progress in Physics* (1996).

6. T. F. Adams, *Astron. Astrophys.* **50**, 461 (1976).

7. J. K. Webb, R. F. Carswell, M. J. Irwin, M. V. Penston, *Mon. Not. R. Astron. Soc.* **250**, 657 (1991).

8. Our first D/H measurement is reported in (2), our second measurement is the subject of this article.

9. A. Songaila, L. L. Cowie, C. J. Hogan, M. Rugers, *Nature* **368**, 599 (1994).

10. R. F. Carswell, M. Rauch, R. J. Weymann, A. J. Cooke, J. K. Webb, *Mon. Not. R. Astron. Soc.* **268**, L1 (1994).

11. K. Jedamzik, G. M. Fuller, *Astrophys. J.* **452**, 33 (1995); K. Jedamzik, G. M. Fuller, G. J. Mathews, *ibid.* **423**, 50 (1994).

12. S. A. Levshakov & W. H. Kegel, *Mon. Not. R. astr. Soc.* **278**, 497-505 (1996).

13. E. M. Hu, T. S. Kim, L. L. Cowie, A. Songaila, *Astron. J.* **110**, 1526 (1995); D. Kirkman and D. Tytler, *Astrophys. J.* in press.

14. C. C. Steidel, *ibid.* **74**, 37 (1990).

15. M. Donahue and J. M. Shull, *Astrophys. J.* **383**, 511 (1991); W. D. Mathews and G. Ferland, *ibid.* **323**, 456 (1987).

16. M. G. Edmunds, *Mon. Not. R. Astron. Soc.* **270**, L37 (1994); N. Hata, R. J. Scherrer, G. Steigman, D. Thomas, T. P. Walker, S. Bludman, P. Langacker, *Phys. Rev. Lett.* **75**, 3977 (1995).

17. J. L. Linsky, A. Diplas, B. E. Wood, A. Brown, T. R. Ayres, B. D. Savage, *Astrophys. J.* **451**, 335 (1995).

18. G. Steigman, & M. Tosi, *Astrophys. J.* **453**, 173 (1995); G. Steigman, & M. Tosi, *Astrophys. J.* **401**, 150 (1992); B. D. Fields *ibid.* **456**, 478 (1996).

19. M. Rugers and C. J. Hogan, *Astrophys. J.* in press (1996).

20. The model presented by Rugers & Hogan (19) is a poor fit to the data in several places: D I Lyα , H I Lyγ and Lyδ blue wing and central spike, and high order lines at 3974, 3972, 3962.5, 3961,3959.5, 3954.8 Å.

21. G. Steigman *Mon. Not. R. Astron. Soc.* **269**, L53 (1994).

22. E. J. Wampler, G. M. Williger, J. A. Baldwin, R. F. Carswell, C. Hazard, R. G. McMahon, *Astron. Astrophys.* in press (1996).

23. R. F. Carswell *et al.*, *et al. Mon. Not. R. astr. Soc.* **278**, 506 (1996).

24. J. C. Mather et al., *Astrophys. J.* **420**, 439 (1994).

25. M. Persic and P. Salucci, *Mon. Not. R. Astron. Soc.* **258**, 14 (1992).

26. B. E. J. Pagel, E. A. Simonson, R. J. Terlevich, M. G. Edmunds, *Mon. Not R. Astron. Soc.* **255**, 325 (1992).

27. K. A. Olive and G. Steigman, *Astrophys. J. Suppl. Ser.* **97**, 49 (1995).

28. Thuan, T. X., Izotov, Y. I., & Lipovetsky, V. A. in "Interplay between massive star formation, the ISM and galaxy evolution", ed. D. Kunth, B.Guiderdoni, M. Heydari-Malayeri & T. X. Thuan, (Gif-sur-Yvette: Editions Frontieres) (1996).

29. R. T. Rood, G. Steigman, B. M. Tinsley, *Astrophys. J.* **207**, L57 (1976); E. Vassiliadis & P. R. Wood, *ibid.* **413**, 641 (1993).

30. Rood, R.T., Bania, T.M. & Wilson, T.L. 1992 *Nature*, **355**, 618.

31. D. Galli, F. Palla, F. Ferrini, U. Penco, *ibid.* **443**, 536 (1995).

32. K. A. Olive, R.T. Rood, D.N.Schramm & J. Truran & E. Vangioni-Flam 1995 *Astrophys. J.*, **444**, 680 (1995).

33. F. Spite and M. Spite, *Astron. Astrophys.* **115**, 357 (1982); M. Spite, F. Spite, J. P. Maillard, *ibid.* **141**, 56 (1984).

34. R. Rebolo, J. E. Beckman, P. Molaro, *ibid.* **192**, 192 (1988); L. Hobbs and C. Pilachowski, *Astrophys. J.* **326**, L23 (1988).

35. J. A. Thorburn, *ibid.* **421**, 318 (1994).

36. S. G. Ryan, T. C. Beers, C. P. Deliyannis, J. A. Thorburn, *ibid.* **458**, 543 (1996); C. P. Deliyanis, S. G. Ryan, T. C. Beers, J. A. Thorburn, *ibid.* **425**, L21 (1994).

37. M. Pratt *et al.*, (MACHO collaboration), "Workshop on Dark Matter in the Universe", Santa Monica, February (1996)

38. D. Zaritsky & S.D.M. White *Astrophys. J.*, 435, 599 (1994).

39. White, S. D. M., Navarro, J. F., Evrard, A. E., & Frenk, C. S. Nature 366, 429 (1993); M. Markvevitch, R. Mushotzky, H. Inoue, K. Yamashita, A. Furuzawa, Y. Tawara, *Astrophys. J.* **456**, 437 (1996).

40. We add or subtract all three errors to give the largest range for Ω_b.

41. A. Linde, "Recent Progress in Inflationary Cosmology", 1st RESCEU inter. Symp., Tokyo, Nov. (1995).

42. R. F. Carswell, J. K. Webb, J. A. Baldwin, B. Atwood, *Astrophys. J.* **319**, 709 (1987) includes a description the VPFIT code which we used to fit absorption lines.

43. S. S. Vogt *et al., Proc. SPIE* **2198**, 362 (1994).

44. J. Mould, *et al.*, *Astrophys. J.* **449**, 413 (1995).

45. We are very grateful to W.M. Keck foundation for their generous gift to science. We would like to thank R.F. Carswell and T. Barlow for providing software which made our analysis possible. We thank Wayne Wack, Meg Whittle, Randy Campbell, and Keith Baker for their assistance in obtaining the data presented here. We thank George Fuller, Bernard Pagel, Max Pettini, Alvio Renzini, Sean Ryan for important science discussions and suggestions.

This preprint was prepared with the AAS LaTeX macros v4.0.

1. Figure Captions

Figure 1: Velocity plots of Lyman α, β, γ (left), and all the metal lines (right) in the absorption system towards QSO 1009+2956 ($z_{em} = 2.616$, V=16). Zero velocity corresponds to the redshift $z = 2.503571$, of the blue component. The vertical dotted lines also show the red component at 2.503704. The histogram represents the observed counts in each pixel normalized to the quasar continuum. The smooth curve show the best fitting Voigt profiles convolved with the instrumental resolution (42). The Lyman lines and Si III (1206) are in the Lyman alpha forest region where there is additional absorption which we do not fit.

On the nights of December 27, 28 1995, we obtained 5.9 hours of spectra with the HIRES echelle spectrograph on the 10-m W. M. Keck Telescope (43). Two exposures of 2.5 and 2 hours covered 3540 – 5530 Å, while a third 1.4 hour covered 3165 – 4370 Å. A 1.14 arcsec slit produced spectra with resolution of 8 kms^{-1}. Each exposure was accompanied by dark, quartz lamp, and Throium-Argon arclamp exposures. A standard star was observed to trace the echelle orders and remove the blaze response in the spectra. We used our standard data reduction (2).

Figure 2: The Lick Spectrum of QSO 1009+2956 shows the Lyman Limit due to the absorber at $z = 2.504$. On November 28, 1995 we used the Kast spectrograph on the Lick 3-m telescope to obtain 1.9 hours of integration covering 3100 Å- 5950 Å. The spectra were calibrated to vacuum heliocentric wavelengths, and optimally extracted.

The smooth line shows the convolved Voigt proflies of the higher order Lyman lines calculated with the parameters in Table 1. The optical depth, measured by the ratio of flux blueward and redward of 3200 Å, constrains the total column density of neutral hydrogen.

Figure 3: A representation of the flow of information in the standard cosmological model. Boxes show measurements, and circles show theories and derived quantities. Most references to quantities shown are discussed in the text. The range for the Hubble Constant, H_0, is taken from Mould et al. (44). When two numbers are shown, one is for $h = 0.98$ and the other is $h = 0.64$. When Ω_b is used, we add or subtract all three errors to enlarge the range.

Figure 4: The BBNS predicted primordial abundances of D and ^{3}He as a function of η and $\Omega_b\, h^2$ (5). The lower two rectangles are defined by the 1σ random plus systematic errors on D/H towards Q1009+2956 and Q1937–1009. The shaded region is from our mean D/H value, with 1σ random errors from the quadratic sum of our random error plus the σ nuclear error. We then add on the systematic error. The upper limit shows D/H towards Q0014+8118.

Figure 5: As Figure 4 but for Y_p, the mass fraction of ^{4}He. Dashed rectangles show the bounds (1σ statistical plus systematic errors) from recent measurements of ^{4}He (26,28). The lack of intersection with the shaded region illustrates the inconsistency of D/H with Helium-4 measurements. The lower rectangle represents the estimates of ^{4}He deduced by Pagel et als., and it includes in its range a systematic underestimation of Y_p of 0.004.

Figure 6: As Figure 4 but ^{7}Li/H The Spite and Thorburn ^{7}Li plateau from measurements of population II stars are shown as dashed and dot-dashed lines respectively. (33,35). Significant depletion of the surface ^{7}Li abundance is the likely source of the discordances. (36). The dotted line shows upper limits from lithium measurements in population I stars.

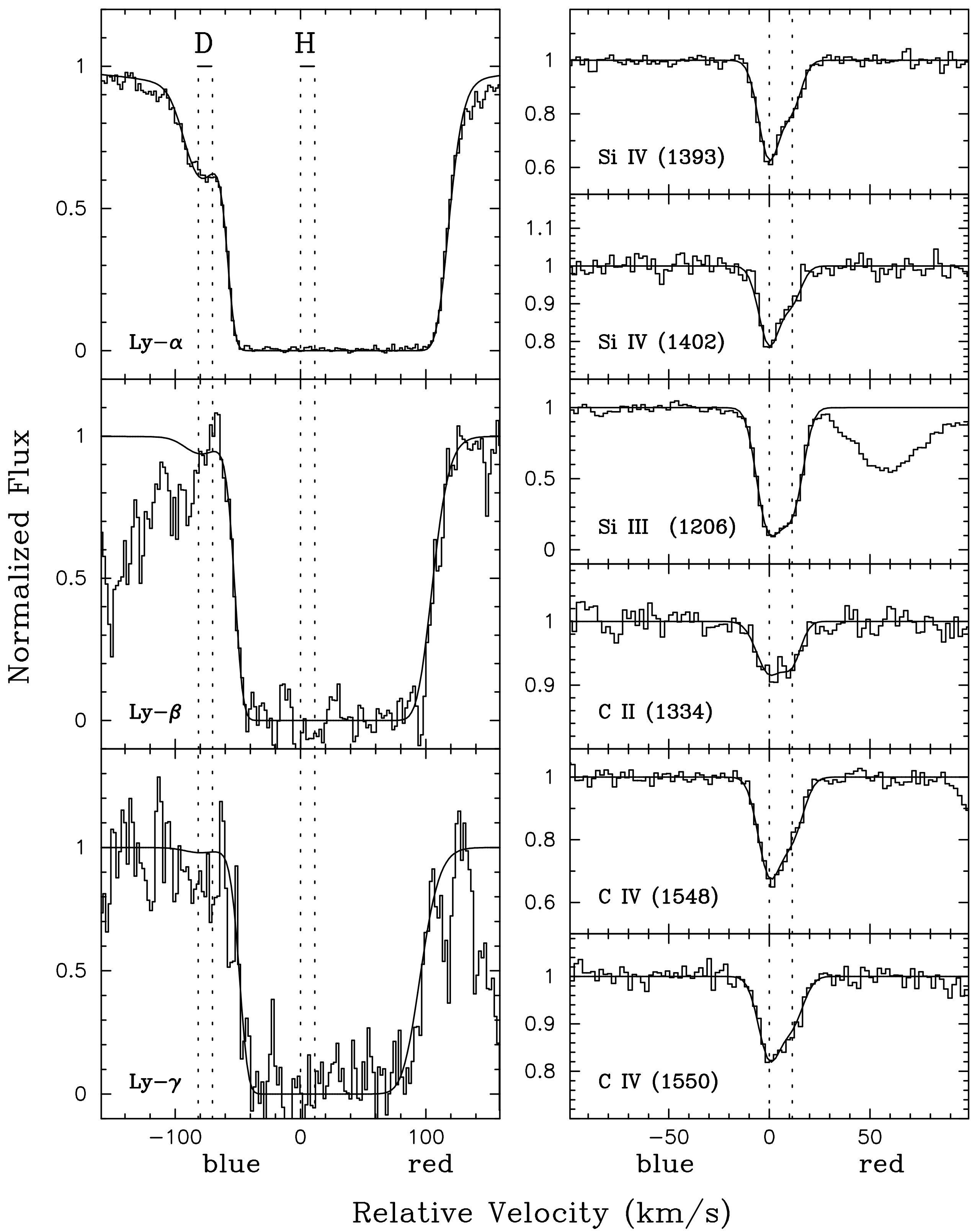
D
H
Ly−α
Ly−β
Ly−γ
Si IV (1393)
Si IV (1402)
Si III (1206)
C II (1334)
C IV (1548)
C IV (1550)
Normalized Flux
−100
0
100
−50
0
50
blue
red
blue
red
Relative Velocity (km/s)

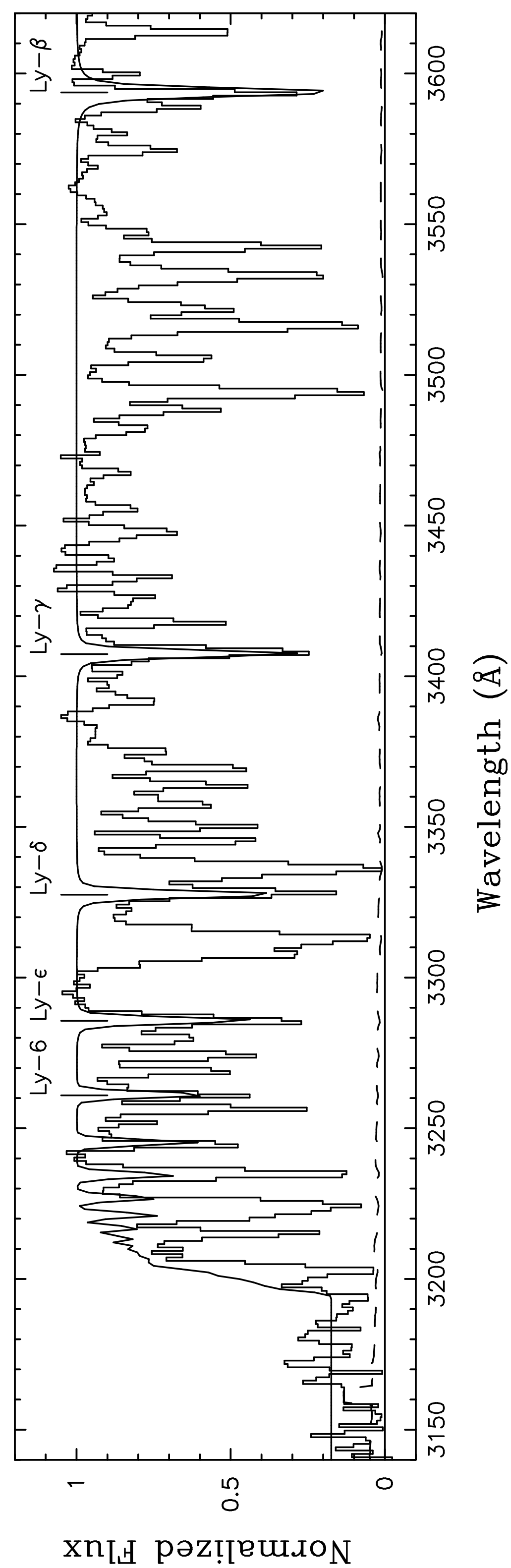

Ly−β
Ly−γ
Ly−δ
Ly−ϵ
Ly−6
Normalized Flux
0
0.5
1
Wavelength (Å)
3150
3200
3250
3300
3350
3400
3450
3500
3550
3600

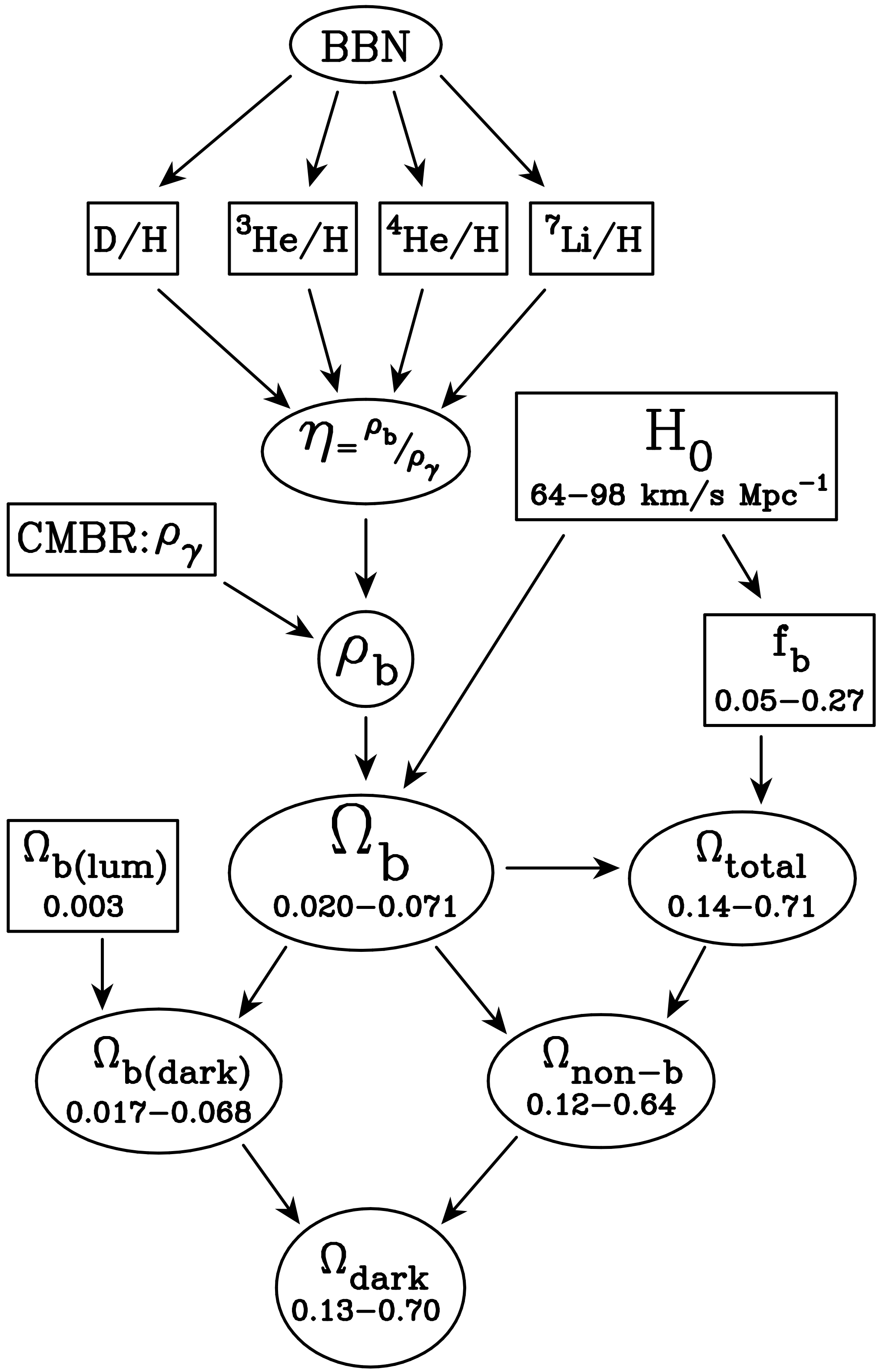
BBN
D/H
^{3}He/H
^{4}He/H
^{7}Li/H
$\eta = \rho_b/\rho_\gamma$
H_0
64−98 km/s Mpc^{-1}
CMBR: ρ_γ
ρ_b
f_b
0.05−0.27
$\Omega_{b(lum)}$
0.003
Ω_b
0.020−0.071
Ω_{total}
0.14−0.71
$\Omega_{b(dark)}$
0.017−0.068
Ω_{non-b}
0.12−0.64
Ω_{dark}
0.13−0.70

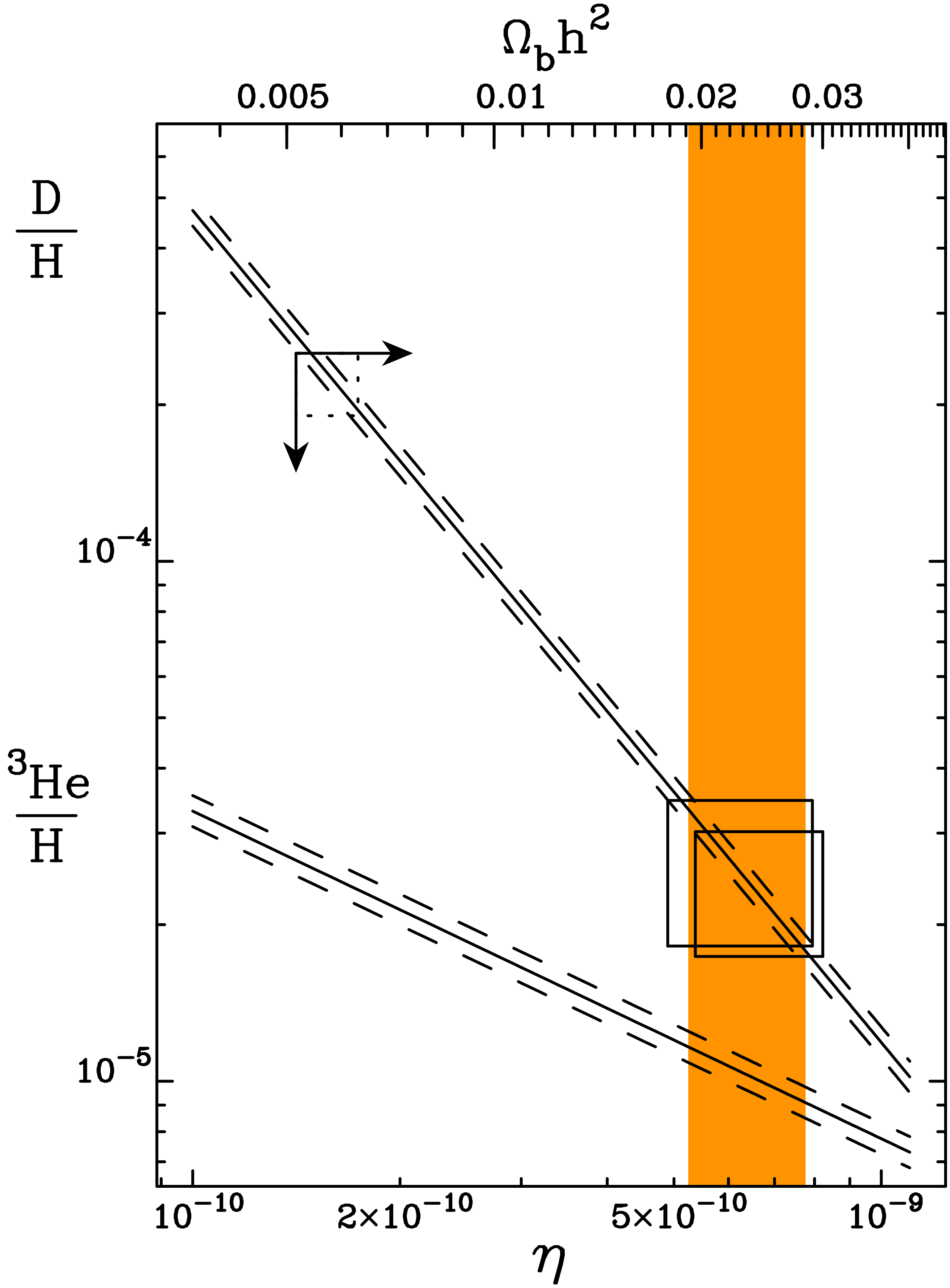

$\Omega_b h^2$
0.005
0.01
0.02
0.03
$\frac{D}{H}$
10^{-4}
$\frac{^3He}{H}$
10^{-5}
10^{-10}
2×10^{-10}
5×10^{-10}
10^{-9}
η

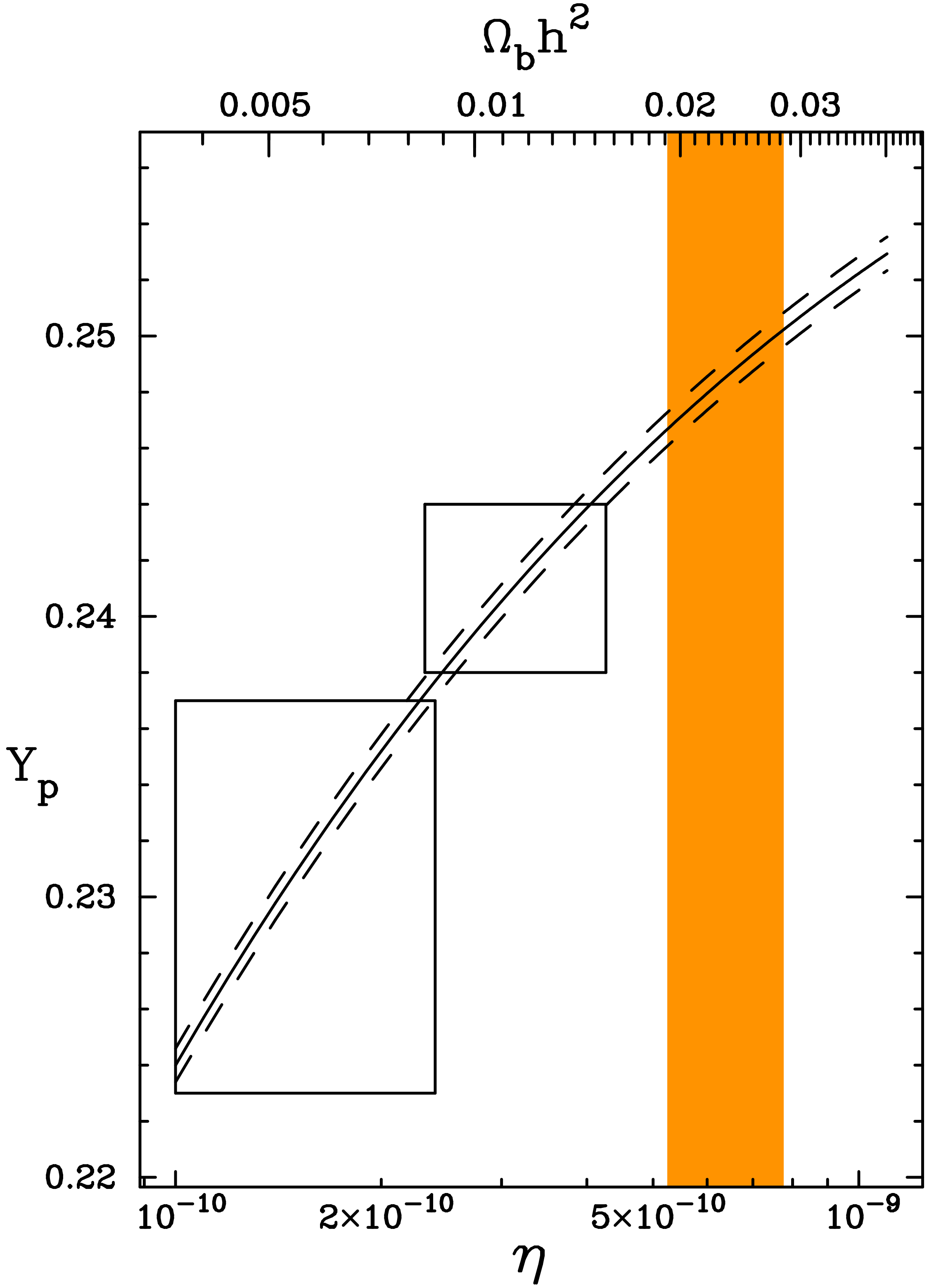
$\Omega_b h^2$
0.005
0.01
0.02
0.03
0.25
0.24
0.23
0.22
Y_p
10^{-10}
2×10^{-10}
5×10^{-10}
10^{-9}
η

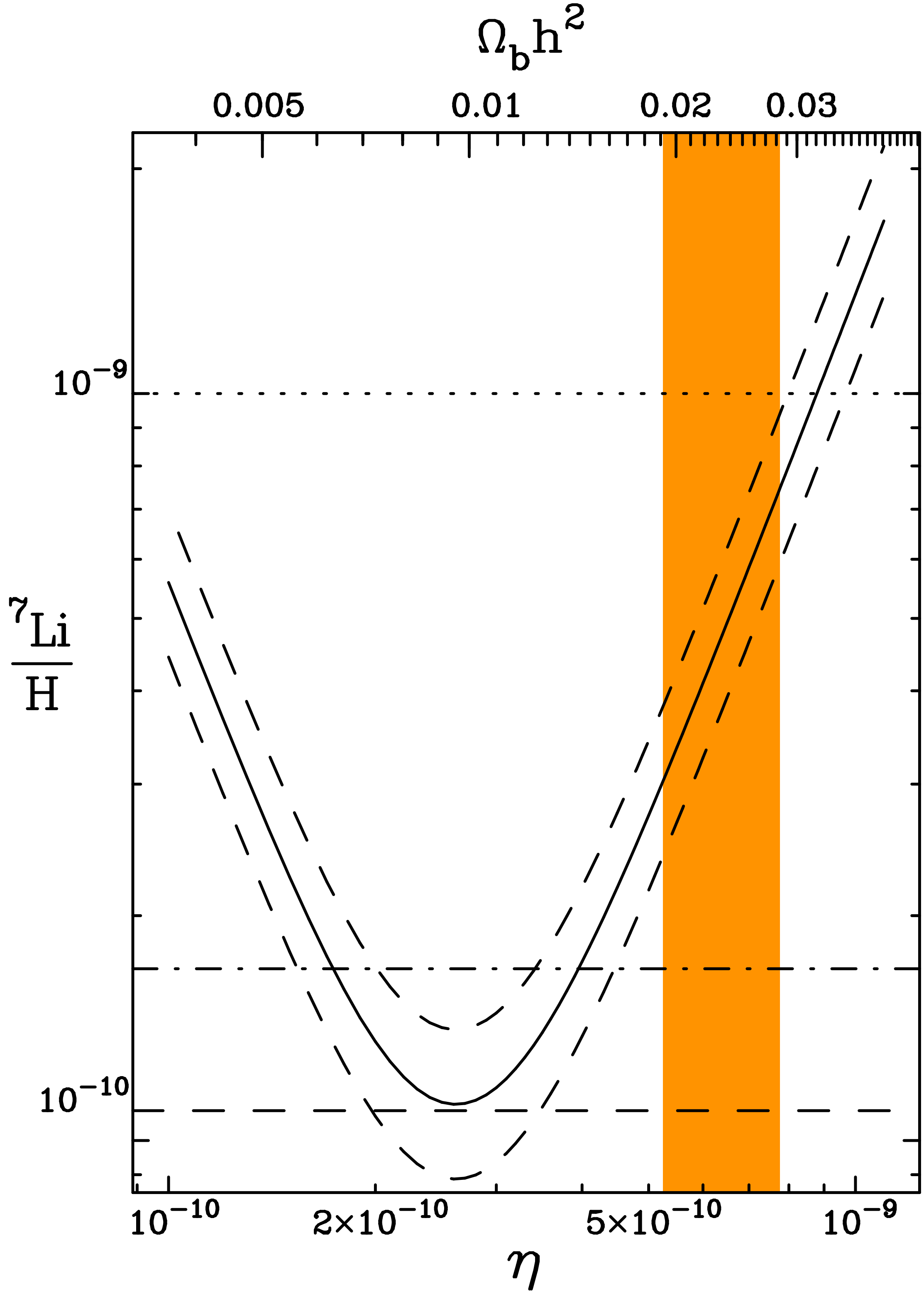

$\Omega_b h^2$
0.005
0.01
0.02
0.03
10^{-9}
10^{-10}
$\frac{^7\mathrm{Li}}{\mathrm{H}}$
10^{-10}
2×10^{-10}
5×10^{-10}
10^{-9}
η